

Equation of State for DNA Liquid Crystals: Fluctuation Enhanced Electrostatic Double Layer Repulsion

H. H. Strey, V. A. Parsegian, and R. Podgornik

National Institutes of Health, DIROD/National Institutes of Diabetes and Digestive and Kidney Diseases, and Laboratory of Structural Biology/Division of Computer Research and Technology, Building 12A/2041, 12 South Dr MSC 5626, Bethesda, Maryland 20892-5626

(Received 30 September 1996)

We have measured the equation of state for DNA solutions at different ionic strengths covering 5 orders of magnitude in DNA osmotic pressure. At high osmotic pressures the equation of state is independent of the ionic strength and is dominated by exponentially decaying hydration repulsion. At lower pressures the equation of state is dominated by screened electrostatics. We also found a fluctuation-enhanced repulsion with a decay length of 4 times the Debye screening length. We present arguments that the form of the fluctuation part of the osmotic pressure is due to the coupling between bending fluctuations and the compressibility of the nematic array normal to the average director. [S0031-9007(96)02279-X]

PACS numbers: 61.30.-v, 64.30.+t, 87.15.Da

Liquid crystals of DNA are the simplest model systems for DNA packing in certain cell nuclei such as in dinoflagellates or in phase heads [1]. In these systems typically a few extremely long (from 10 μm up to 1 m) DNA molecules form a macroscopic liquid crystal. Long DNA molecules can do this because their length exceeds by far the DNA persistence length and can therefore fold back on itself. Recently, DNA has attracted some attention as a model polymer for studying fundamental liquid crystalline physics. The advantages of DNA over many synthetic polymers are various: By using modern molecular biological methods monodisperse DNA solutions can be prepared with a wide variety of lengths (from nm up to cm); DNA has a persistence length of about 50 nm, nicely placed in the accessible length range; DNA is soluble in water; DNA is charged ($2e^-/3.4 \text{ \AA}$) making it a good candidate to study polyelectrolyte behavior; in monovalent salt solutions DNA-DNA interactions are dominated purely by repulsive forces (attractive forces could lead to a collapse of the DNA without any applied force). Additional interest in the physics of DNA arrays comes from the close analogy to the physics of magnetic flux line arrays in type II superconductors [2]. Although lyotropic polymer liquid crystalline phases have been known for quite some time, not very much is known either experimentally or theoretically about their equations of state (osmotic pressure Π vs V_{polymer}). Most work has been focused on the location and order of phase boundaries [3]. Using osmotic stress to set the chemical potential of DNA we have recently investigated the energetics of compacting long ($>10 \mu\text{m}$) DNA molecules into liquid crystals [4]. In this paper we present measurements of the equation of state of long DNA molecules over 5 orders of magnitude in applied osmotic stress. For the first time, it is possible to determine free energy changes incurred in going from an isotropic phase, through various chiral phases, into a nonchiral line hexatic phase, then all the way up to the hexagonal phase.

At high DNA densities, the contribution of the configurational entropy of the polymer lattice to the osmotic pressure is negligible; the osmotic pressure is directly related to the interaxial forces dominated by hydration repulsion. There is an exponential decay with a characteristic length of 3 \AA . In this regime of DNA densities, the equation of state is independent of the ionic strength of the buffer. At lower DNA densities, in addition to direct electrostatic double layer repulsion between charged rods, an exponential force with Debye screening length λ_D , we also found fluctuation-enhanced repulsion with a decay length of 4 times λ_D . The osmotic pressure in this regime has contributions from both bare interaxial forces as well as from bending fluctuation forces, similar to Helfrich forces in smectic arrays [5]. We suggest reasons why the form of the fluctuation part of the osmotic pressure is due to the coupling between bending fluctuations and the compressibility of the nematic array normal to the average director.

Long ($M_w > 10^8$) DNA was prepared from whole adult chicken blood (Truslow Farms, Chestertown, MD) following [6]. At high osmotic pressures (10^8 – $10^{5.8}$ dyn/cm²), DNA unoriented (powder) samples (0.4 mg DNA) were equilibrated in vast excess against various solutions of polyethyleneglycol (PEG 8000 M_w or PEG 20 000 M_w , from Fluka Chemicals) in either 100 mM, 0.5 M, or 1 M NaCl; 10 mM Tris, 1 mM EDTA, pH 7 as described in [4]. Under these conditions, PEG (20 000 M_w) is completely excluded from the DNA phase for concentrations greater than 7% ($w_{\text{PEG}}/w_{\text{water}}$). The equilibration time was usually from 4 days to a week. The interaxial spacing between DNA molecules, and consequently the density of these samples, was determined by small angle x-ray scattering as described in [4]. In the cholesteric regime ($d_{\text{int}} > 35 \text{ \AA}$) an Elliot GX-13 Rotating Anode x-ray generator equipped with two x-ray mirrors and a Franck-type camera was used. Image plates were scanned and digitized by

a phosphor imager SI (Molecular Dynamics, CA); the radial scattering intensity $I(q)$ was determined by image processing using NIH IMAGE version 1.60 (W. Rasband, NIH, Bethesda, MD) modified by us. After subtracting background scattering, the scattering intensity was fitted to a powder-averaged Lorentzian times the solid-cylinder form factor $F(q)$ for Na-DNA that has been determined by solution x-ray scattering [7]. Below osmotic pressures of $10^{5.8}$ dyn/cm², the stressing polymer (PEG 20 000M_w) does not remain phase separated from the DNA array, and an exclusion must be enforced externally. For this reason DNA samples at lower osmotic pressures ($10^{5.5}$ – 10^4 dyn/cm²) were prepared in dialysis tubes (SpektraPor Cellulose Ester 10,000 MWCO, Spektrum) bathed in Dextran T110 (Fluka) solutions of various concentrations [25%–1%(w/w_{water})] at salt concentrations of 100 mM, 0.5 M, or 1 M NaCl; 10 mM Tris, 1 mM EDTA, pH 7. For this regime we chose Dextran over PEG as a stressing agent, because Dextran is a branched polysaccharide whose shape prevents passage through semipermeable membranes of reasonably small molecular weight cutoff (<10 000). Also the osmotic pressure of Dextran solutions has been measured down to much lower osmotic pressures [8]. The dialysis tubes were filled with 2 ml of dilute DNA solutions (5–10 mg/ml DNA), so that the process of osmotic equilibrium always concentrated the DNA solution. In order to reduce the equilibration time, we matched the salt concentrations inside and outside. The samples were then equilibrated in 200 ml stressing solution for 2–4 weeks, during which they were stirred once a day. After equilibrium, the samples were quickly transferred into plastic tubes and then weighed using a high precision balance (Mettler, NJ). The samples were then dried in vacuum and then weighed again. The dry DNA, salt mixture was then dissolved into a known amount of buffer (10 mM Tris, 1 mM EDTA, pH 7) to measure the total amount of DNA by determining the absorbance at 260 nm ($c_{\text{DNA}} = 50 \mu\text{g/ml } A_{260}$). With this method we could independently determine the amount of water, salt, and DNA in these samples.

In Fig. 1 we plot $\log_{10} \partial G / \partial d$ versus effective interaxial spacing d at an ionic strength of 500 mM NaCl, where G is the free energy per unit length ($\partial G / \partial d = \Pi_{\text{osm}} \sqrt{3} d$, assuming hexagonal packing [9]). We chose to plot $\log_{10} \partial G / \partial d$ versus intermolecular distance because we expected the dominant repulsive interactions to be exponential (hydration and screened electrostatics). At high osmotic pressures the $\partial G / \partial d$ curve could be well fitted with an exponentially decaying force of about 3 Å decay length, typical for structural forces in water (hydration forces) [10]. The samples in regime *a* are in a long-range bond-ordered, but short-range positionally ordered phase [4] [line hexatic, Fig. 1(a)]. In regime *b*, we found two x-ray diffraction maxima [11]: a sharper peak (continuing regime *a*) at smaller interaxial spacings and a more diffuse one at wider spacings (continued by regime *c*). At lower osmotic pressures (regime *c*), the fitted decay

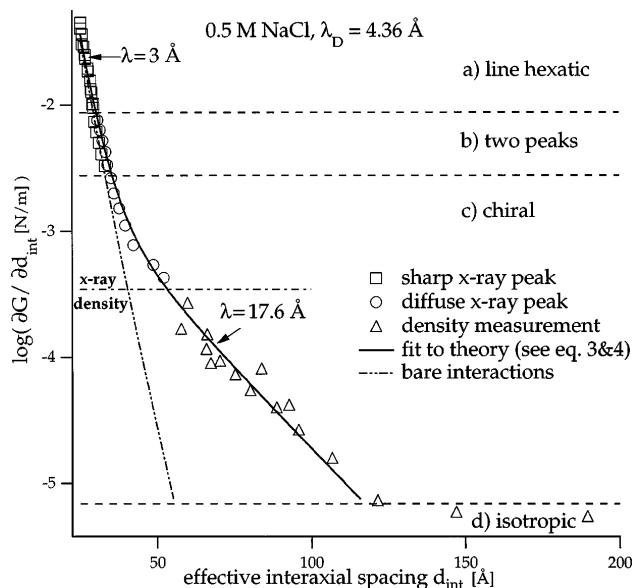


FIG. 1. Equation of state for DNA at an ionic strength of 0.5 M NaCl. We plotted $\log_{10}(\partial G / \partial d)$ versus effective interaxial spacing d . Four structural regimes *a*–*d* could be distinguished. The solid curve represents a fit of the data points from regimes *a*–*c* to a nematic liquid crystalline theory (see text) assuming exponential repulsion (hydration and screened electrostatics). The broken line represents the bare interaction without fluctuation enhanced repulsion. Interaxial spacings above the $- \cdot -$ line are measured by x-ray scattering; below this line the spacing d are derived from measured DNA densities, where molecules are expected to be hexagonally packed.

length was found to depend on the ionic strength of the solution. In 0.5 M NaCl solutions ($\lambda_D = 4.36$ Å), there was no extended linear regime decaying with λ_D . Instead, after a short intermediate regime, we saw a decay length of $\lambda = 17.6$ Å, 4 times λ_D (regime *c*). At even lower pressures (*d*) the curve flattens again, when the DNA solution turns isotropic. In 100 mM NaCl ($\lambda_D = 9.74$ Å, data not shown), after the initial hydration regime, we found an extended exponential regime with a decay length of 10 Å, which flattens further at lower pressures down to a decay length of approximately 40 Å. In 1 M NaCl ($\lambda_D = 3.08$ Å, data not shown) an extended exponential regime with a decay length of 14 Å was observed, after which the solutions turned isotropic.

Before presenting our tentative interpretation of these data, to encourage more careful thinking about real systems with real interactions, we have plotted the data in two different ways; we will speak of two different forms—exponential or power-law—for the equation of state. Sometimes with different language, different interpretations emerge.

Since DNA is a semiflexible polyelectrolyte (the stiffness of DNA originates mainly from its double helical conformation and not from the charge density along the chain), one expects the equation of state to depend on the ionic strength of the bathing solution. Often the

polyelectrolyte character of molecules is incorporated in liquid crystalline theory by adding a Debye screening length to the hard core diameter of the molecule. But this procedure is obviously dangerous, because it assumes that the equation of state at different ionic strengths can be described by the same power law, an unavoidable consequence of hard core interactions. Figure 2 shows a $\log_{10}(\Pi)$ vs $\log_{10}(1/\text{density})$ plot for three different ionic strengths (100 mM, 500 mM, and 1 M NaCl). The solid lines represent linear fits over different regimes with the corresponding negative slopes indicated by arrows. At high pressures, where the equation of state seems not to depend on ionic strength, all data can be fitted by a V^{-5} power law. At lower pressures the fitted slopes vary somewhat with the ionic strength of the bathing solution ($V^{-3.2}$ for 1 M NaCl, $V^{-3.0}$ for 0.5 M NaCl, and $V^{-2.7}$ for 100 mM NaCl). In this regime all observed slopes differ qualitatively from the theoretically predicted power laws for hard core repulsion (Harbich-Helfrich: $\Pi \propto V^{-4/3}$ for hexagonal crystals [12], and Selinger-B Bruinsma: $\Pi \propto V^{-5/3}$ for nematics [13]). A hard core picture does not work here.

An alternative way to present the data has been already shown in Fig. 1 for 0.5 M NaCl. By plotting $\log_{10} \partial G / \partial d$ versus intermolecular distance exponential behavior is emphasized. After the line hexatic and the coexistence regime (Fig. 1, regimes *a* and *b*), the curve

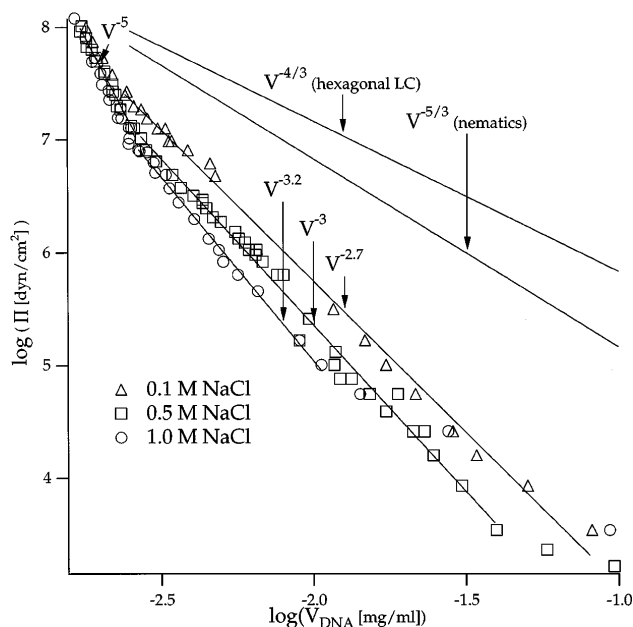


FIG. 2. Double-logarithmic plot of the equation of state (Π vs V_{DNA}) for DNA at ionic strengths of 100 mM (Δ), 0.5 M (\square), and 1 M (\circ) NaCl. The solid lines represent linear fits over different regimes with the corresponding negative slopes indicated by arrows. At lower pressures the fitted slopes varied with the ionic strength of the bathing solution ($V^{-3.2}$ for 1 M NaCl, $V^{-3.0}$ for 0.5 M NaCl, and $V^{-2.7}$ for 100 mM NaCl) with powers clearly inconsistent with that expected from universal scaling behavior. Volumes V_{DNA} at higher Π are derived from interaxial spacings measured by x-ray scattering.

slowly deviates from a single exponentially decaying force with a decay length of 3 \AA . In this intermediate regime the slope varies continuously from 3 \AA to about 5 \AA . In regime *d*, however, the curve turns into an extended linear regime with an exponential decay length of 17.6 \AA . Though a transitional regime with a decay length between λ_D and $4\lambda_D$ is clearly visible (Fig. 1), we were unable to identify an extended regime with a decay length of $2\lambda_D$ as reported in some of our previous works [14]. The x-ray diffraction analysis used in this work differs from previous procedures in the cholesteric regime. Instead of taking the maximum in the diffraction pattern, we fitted the whole radial intensity profile $I(q)$ using a powder-averaged Lorentzian structure factor and an independently measured form factor for Na-DNA. The reason for the resulting difference in interaxial spacings is that at lower osmotic pressures the diffraction maxima become quite broad and fluidlike. Since the scattering intensity $I(q)$ is the product of the structure factor $S(q)$ and the form factor $|F(q)|^2$ of DNA, the maximum of $I(q)$ differs from the maximum of the structure factor $S(q)$.

The absence of a doubling of the screening length may not be surprising, since we deal with a nematiclike system, where the cholesteric pitch makes only a small contribution to the free energy. All theoretical calculations that predicted regimes where the exponential decay length is doubled and then quadrupled assumed crystalline structure [13,14]. To first approximation, nematic polymeric liquid crystals can be described by a Hamiltonian of the form [2,15]:

$$H = H_0(d) + \frac{1}{2} \sum_q (K_2 q_\perp^2 + K_3 q_z^2) |n^T(q)|^2 + \frac{1}{2} \sum_q \left[K_1 q_\perp^2 + K_3 q_z^2 + \frac{q_\perp^2}{q_z^2} k_B T \rho_0^2 A(q) \right] |n^L(q)|^2. \quad (1)$$

$H_0(d)$ is the direct energy (bare interactions) needed to bring the molecules to their average interaxial distance d ; the second term represents conformational fluctuations expressed in terms of n^T and n^L , the transverse and longitudinal components of deviations away from the average nematic director along the z axis. K_1 , K_2 , K_3 are the Frank constants for splay, twist, and bending, and $A(q)$ describes the free energy contribution due to the fluid nature of the system. The limit of $A(q_\perp \rightarrow 0, q_z = 0) = B/k_B T \rho_0^2$, for example, results in the bulk modulus B for compressions and dilations normal to the chains.

Within this formalism we consider the following possibility. Again to first approximation, the Frank constants K_1 , K_2 , K_3 as well as the bulk modulus B should vary with spacing as does the bare interaction between chains. This is an exponential decay. However, since each DNA molecule has an intrinsic bending stiffness κ , the bulk bending modulus K_3 should at some spacing lose its dependence on interaction and cross over to a simple bending density modulus $\kappa \rho_{\text{DNA}}$, where ρ_{DNA} is the cross-sectional density of molecules. This is because K_3 will

come to be dominated by the work of bending a bundle of molecules with little extra work from exponentially weakened molecular interactions. At the same time, K_1 , K_2 , and B continue to decrease exponentially with increasing distance between molecules. This has a powerful consequence at low densities where K_3 comes to dominate the moduli. Looking at the fluctuation part of the free energy, it can be shown that in the limit of $K_1 \ll K_3$ the fluctuation part is dominated by

$$G - H_0 \propto \sqrt[4]{\frac{B}{K_3}} \propto e^{-d/4\lambda_D}. \quad (2)$$

There exists a dense regime where the free energy G scales as the bare interactions with e^{-d/λ_D} and a dilute regime where G scales as $e^{-d/4\lambda_D}$. Because this regime is due to fluctuations around the equilibrium, we call this second part of the free energy "fluctuation enhanced repulsion," in analogy with Helfrich's steric repulsion in smectic arrays [5]. The major difference from his system is that in our case the dominating interaction is not steric, but exponential. It has to be emphasized that not only the strength of the bare repulsion but also its range is enhanced by fluctuations. Figure 1 shows that interactions in DNA solutions are dominated by exponential repulsion over a range of almost 30 times its bare decay length ($\lambda_D = 4.36 \text{ \AA}$). This is at least an order of magnitude larger than one expects to be able to see. The results can be explained consistently from the reasoning behind Eq. (2). DNA shows two bare repulsive interactions: hydration repulsion ($\lambda_H = 3 \text{ \AA}$) and screened electrostatics (λ_D). These go as $K_0(d/\lambda)$, which at large distances d can be accurately approximated by $\sqrt{\pi/2}(e^{-d/\lambda}/\sqrt{d/\lambda})$.

$$H_0(d) = a \frac{e^{-d/\lambda_H}}{\sqrt{d/\lambda_H}} + b \frac{e^{-d/\lambda_D}}{\sqrt{d/\lambda_D}} \quad (3)$$

$$\frac{\partial G}{\partial d}(d) = \frac{\partial}{\partial d} H_0(d) + ck_B T \kappa^{-1/4} \frac{\partial}{\partial d} \sqrt[4]{\frac{\partial^2 H_0}{\partial d^2}}, \quad (4)$$

using $B \approx \partial^2 H_0 / \partial d^2$. From this we might see two distinct regimes with decay length of λ_H and λ_D , as well as regimes where the fourth root of B essentially quadruples the screening length. In fact, the solid line in Fig. 1 was obtained by fitting the experimental $\partial G / \partial d$ to Eqs. (3) and (4) with decay length of $\lambda_H = 3 \text{ \AA}$ and λ_D , using three fit parameters a , b , and c (100 mM: $a = (6.9 \pm 1.9) \times 10^{-8} \text{ J/m}$, $b = (3.5 \pm 0.3) \times 10^{-10} \text{ J/m}$, $c = 0.8 \pm 0.06$; 0.5 M: $a = (8.9 \pm 3.7) \times 10^{-8} \text{ J/m}$, $b = (3.1 \pm 2.8) \times 10^{-9} \text{ J/m}$, $c = 1.2 \pm 0.3$; 1 M: $a = (9.7 \pm 0.5) \times 10^{-8} \text{ J/m}$, $b = 0$, $c = 1.1 \pm 0.1$). For both 1 M and 0.5 M NaCl the hydration and Debye screening lengths are very close; the hydration interaction with its larger amplitude wins. At low pressures, the interaction with the longest decay length survives, that is, $4 \times \lambda_D$. In 100 mM NaCl so-

lutions λ_H and λ_D are different enough that the bare screened electrostatic repulsion could be observed.

The ability to measure an equation of state and to map the phase diagram for free energies creates an opportunity, and even an obligation, to test liquid crystalline theories more carefully than has been possible before. A full analysis will combine all available information about phase transitions and structure of the different phases together with these measured changes in free energy.

We want to thank Don Rau, David Nelson, and Robijn Bruinsma for fruitful discussions and Gary Melvin and Leipo Yu for their support enabling the x-ray experiments. Special thanks to Randy Kamien, who pointed out to us the right form of the Hamiltonian for polymer nematic liquid crystals. One of the authors (H. H. S.) acknowledges financial support by the Deutsche Forschungsgemeinschaft (Str 454/1-2).

-
- [1] F. Livolant, *Physica* (Amsterdam) **176A**, 117–137 (1991).
 - [2] R. D. Kamien, P. Doussal, and D. R. Nelson, *Phys. Rev. A* **45**, 8727 (1992).
 - [3] J. Tang and S. Fraden, *Liq. Cryst.* **19**, 459–467 (1995).
 - [4] R. Podgornik *et al.*, *Proc. Natl. Acad. Sci. U.S.A.* **93**, 4261–4266 (1996), and references therein.
 - [5] W. Helfrich, *Z. Naturforsch.* **33a**, 305–315 (1978).
 - [6] H. Shindo, J. D. McGhee, and J. S. Cohen, *Biopolymers* **19**, 305–315 (1978).
 - [7] S. Bram and W. W. Beeman, *J. Mol. Biol.* **55**, 311–324 (1971).
 - [8] C. Bonnet-Gonnet, L. Belloni, and B. Cabane, *Langmuir* **10**, 4012 (1994).
 - [9] At high osmotic pressures (line hexatic phase) the hexagonal structure has been confirmed by x-ray diffraction. In the low pressure regime the effective intermolecular distance was calculated from the DNA density assuming local hexagonal packing of the DNA molecules. In this regime the hexagonal order is distorted by macroscopic twist (cholesteric and possibly blue phase). This twist extends typically over several hundred intermolecular spacings, so that in these regimes local hexagonal packing can still be used.
 - [10] S. Leikin *et al.*, *Annu. Rev. Phys. Chem.* **44**, 369–395 (1993).
 - [11] Since we hold all intensive variables (p, T, μ) fixed the measured $S(q)$ should originate from a single phase. At this point it is not yet clear whether this structure corresponds to a new phase located between a columnar (nonchiral) and a cholesteric (chiral) arrangement of the DNA molecules.
 - [12] W. Helfrich and W. Harbich, *Chem. Scr.* **25**, 32 (1985).
 - [13] J. V. Selinger and R. F. Bruinsma, *Phys. Rev. A* **43**, 2922–2931 (1991).
 - [14] R. Podgornik and V. A. Parsegian, *Macromolecules* **23**, 2265–2269 (1990).
 - [15] J. V. Selinger and R. F. Bruinsma, *Phys. Rev. A* **43**, 2910 (1991).